

# Synthesis and characterization of uranium trichloride in alkali-metal chloride media

July 2022

Steven D Herrmann, Haiyan Zhao, Kaustubh Krishna Bawane, Lingfeng He, Kevin R Tolman, Xiaofei Pu





### DISCLAIMER

This information was prepared as an account of work sponsored by an agency of the U.S. Government. Neither the U.S. Government nor any agency thereof, nor any of their employees, makes any warranty, expressed or implied, or assumes any legal liability or responsibility for the accuracy, completeness, or usefulness, of any information, apparatus, product, or process disclosed, or represents that its use would not infringe privately owned rights. References herein to any specific commercial product, process, or service by trade name, trade mark, manufacturer, or otherwise, does not necessarily constitute or imply its endorsement, recommendation, or favoring by the U.S. Government or any agency thereof. The views and opinions of authors expressed herein do not necessarily state or reflect those of the U.S. Government or any agency thereof.

# Synthesis and characterization of uranium trichloride in alkali-metal chloride media

Steven D Herrmann, Haiyan Zhao, Kaustubh Krishna Bawane, Lingfeng He, Kevin R Tolman, Xiaofei Pu

**July 2022** 

Idaho National Laboratory Idaho Falls, Idaho 83415

http://www.inl.gov

Prepared for the U.S. Department of Energy Under DOE Idaho Operations Office Contract DE-AC07-05ID14517

# Synthesis and Characterization of Uranium Trichloride in Alkali-Metal Chloride Media

Steven D. Herrmann<sup>a,b,\*</sup>, Haiyan Zhao<sup>b</sup>, Kaustubh K. Bawane<sup>a</sup>, Lingfeng He<sup>a</sup>, Kevin R. Tolman<sup>a</sup>, and Xiaofei Pu<sup>a</sup>

<sup>a</sup> Idaho National Laboratory, Idaho Falls, Idaho, USA

<sup>b</sup> University of Idaho, Idaho Falls, Idaho, USA

\*Corresponding author; Tel: +1 208 533 7859; Email address: Steven.Herrmann@inl.gov;

Postal address: P.O. Box 1625, Idaho Falls, Idaho, 83415-6180, USA

### **Abstract**

Given a growing interest in uranium salts for pyrochemical processing of used fuel and uranium-fueled molten salt reactors, the synthesis of uranium trichloride in alkali-metal chloride media was investigated in a series of four experiments. Specifically, uranium metal powder and uranium hydride powder were prepared and separately blended with ammonium chloride and lithium chloride – potassium chloride eutectic in two runs, while the same powders were separately blended with ammonium chloride and sodium chloride in two additional runs. Each of the lithium chloride – potassium chloride containing blends was slowly heated to 923 K, while those containing sodium chloride were heated to 1123 K. During each heat up, the ammonium chloride sublimed into gaseous ammonia and hydrogen chloride, leading to the chlorination of uranium metal or uranium hydride and the formation of molten salt solutions of the respective chlorides. Experimental conditions were incorporated in the runs to promote formation of uranium trichloride over uranium tetrachloride in the respective media. Molten samples of each run product were taken and characterized via chemical analyses, diffractometry, and microscopy. The final products from each run were dark dense ingots of the respective salt systems with uranium concentrations ranging from 44 to 51 wt%. Chemical analyses and diffractometry identified the predominant presence of uranium trichloride in these systems; however, a possible minor presence of uranium tetrachloride could not be conclusively dismissed.

Key words: Uranium trichloride synthesis, uranium trichloride characterization, uranium metal chlorination, uranium hydride chlorination, ammonium chloride

### 1. Introduction

Uranium trichloride is a unique compound that is primarily used in the electrorefining of uranium metal from impure uranium metal feedstocks. Specifically, in the electrometallurgical treatment of used sodium-bonded fast reactor metallic fuels, a solution of uranium trichloride in lithium chloride – potassium chloride eutectic at about 773 K is utilized as a molten salt electrolyte to electrotransport uranium metal from the used metallic fuel to a refined uranium metal deposit for harvesting and subsequent uranium-235 down blending. [1-3] Additionally, uranium trichloride is a candidate fuel form for use in proposed molten chloride fast reactors. [4]

As uranium trichloride is generally used in a molten salt system with one or more metal chlorides, the user typically synthesizes it for a specific system. In the case of the electrometallurgical treatment process, researchers at Argonne National Laboratory (ANL) detailed a method to synthesize uranium trichloride. [5] This method involved preparing a vessel containing molten cadmium underneath a pool of lithium chloride – potassium chloride eutectic salt at 873 K. A porous basket containing uranium metal was suspended in the salt and rotated. Gaseous chlorine was injected into the cadmium pool, forming cadmium chloride. The cadmium chloride rose through the cadmium layer and into the molten salt pool, where the chloride reacted with uranium in the basket to form uranium trichloride per the following reaction and calculated Gibbs energy change. [6]

$$3/2 \text{ CdCl}_2 + \text{U} \rightarrow \text{UCl}_3 + 3/2 \text{ Cd}$$
  $\Delta G_{Rx.873K} = -293 \text{ kJ}$  (1)

The cadmium metal reaction product sank back into the cadmium pool. After the desired concentration of uranium trichloride (nominally 50 wt% uranium as the trichloride) was reached, the reaction was stopped, and the salt product was pressure siphoned out of the vessel. Despite

the separate cadmium and salt phases in this process, along with subsequent salt distillation operations to purify the product, the LiCl-KCl-UCl<sub>3</sub> product still contained 0.4 wt% cadmium.

While the presence of cadmium in the above-described synthesis of a uranium trichloride salt system was not detrimental to its use in the specified electrometallurgical treatment process, the presence of this toxic metal is undesirable in other applications. Consequently, researchers have investigated similar approaches without using cadmium to synthesize uranium-trichloridebearing salt systems via metal chloride reactions with uranium metal to form uranium trichloride in molten salts. Some of the metal chlorides that were investigated include copper chloride [7], bismuth chloride [8], and zinc chloride [9], per the following respective reactions and calculated Gibbs energy changes. [6]

$$3/2 \text{ CuCl}_2 + \text{U} \rightarrow \text{UCl}_3 + 3/2 \text{ Cu}$$
  $\Delta G_{\text{Rx},873\text{K}} = -535 \text{ kJ}$  (2)

$$BiCl_3 + U \rightarrow UCl_3 + Bi \qquad \Delta G_{Rx,873K} = -463 \text{ kJ}$$
 (3)

$$3/2 \text{ ZnCl}_2 + \text{U} \rightarrow \text{UCl}_3 + 3/2 \text{ Zn}$$
  $\Delta G_{\text{Rx.873K}} = -242 \text{ kJ}$  (4)

However, in each of these cases, further separation of the metal chloride reactant or associated metal reaction product is required to obtain a higher-purity uranium-trichloride-bearing salt system.

Higher-purity forms of uranium chloride could be synthesized by contacting uranium metal directly with chlorine or hydrogen chloride gases, per the following generalized reactions, in lieu of metal chlorides.

$$U + x/2 \operatorname{Cl}_2(g) \to U\operatorname{Cl}_x \tag{5}$$

$$U + x HCl (g) \rightarrow UCl_x + x/2 H_2 (g)$$
 (6)

A challenge with the former reaction (Eq. 5) is that chlorine gas can produce tri-, tetra-, penta-, and hexachloride forms of uranium. [10-11] Furthermore, the corrosive nature of chlorine could introduce contaminants into the product due to interaction with materials of construction. The formation of a reducing hydrogen gas in the latter reaction (Eq. 6) precludes the formation of penta- and hexachloride forms of uranium; however, this reaction favors chlorination of uranium trichloride to the tetrachloride in the presence of excess hydrogen chloride.

Delivery of hydrogen chloride in a solid form to uranium metal can be accomplished with ammonium chloride, which sublimes into gaseous ammonia and hydrogen chloride at 611 K.

This approach offers a potential advantage by not requiring a gas sparging system to introduce gaseous hydrogen chloride. Researchers at the Korea Atomic Energy Research Institute contacted uranium metal pellets with ammonium chloride under heat and observed a mixed uranium trichloride and uranium tetrachloride product along with unreacted uranium metal, despite applying a super-stoichiometric amount of ammonium chloride for the given metal mass.

[12] Additionally, researchers at Oregon State University and ANL [13] contacted uranium metal with an excess of ammonium chloride to produce uranium tetrachloride. The tetrachloride was then blended with uranium metal and heated to 823 K to reduce the tetrachloride to uranium trichloride per the following reaction and calculated Gibbs energy change. [6]

$$3 \text{ UCl}_4 + \text{U} \rightarrow 4 \text{ UCl}_3$$
  $\Delta G_{\text{Rx,823K}} = -410 \text{ kJ}$  (7)

The objective of this experimental study was synthesis of a concentrated uranium trichloride in alkali-metal chloride media at bench scale, where the product would be devoid of contaminants that might otherwise arise from using metal chloride reactants. Specifically, uranium metal powder and uranium hydride powder were contacted separately with ammonium chloride in either sodium chloride or lithium chloride – potassium chloride eutectic under heat to

produce molten salt solutions containing uranium trichloride, per the following anticipated reactions and calculated Gibbs energy changes. [6]

$$U + 3 NH_4Cl \rightarrow UCl_3 + 3 NH_3(g) + 3/2 H_2(g)$$
  $\Delta G_{Rx,611K} = -416 kJ$  (8)

$$UH_3 + 3 NH_4Cl \rightarrow UCl_3 + 3 NH_3(g) + 3 H_2(g)$$
  $\Delta G_{Rx,611K} = -403 kJ$  (9)

The ammonium chloride was delivered sub-stoichiometrically for a given mass of uranium feed material to promote the formation of uranium trichloride over uranium tetrachloride per Eq. 7. Furthermore, the bench-scale experiments were conducted using materials that were compatible with a chlorinating environment to prevent impurity introduction into the product.

# 2. Experimental Aspects

### 2.1 Approach

The approach for this experimental study was based on production of a eutectic mixture of uranium trichloride and sodium chloride (i.e., NaCl – 32 mol% UCl<sub>3</sub>), which has a eutectic melting point of 798 K, [14] while the melting point for a similarly proportioned mixture of the ternary salt (40 mol% LiCl – 29 mol% KCl – 31 mol% UCl<sub>3</sub>) was expected to be approximately 748 K. [15] The scale of this experimental study was limited to uranium metal feeds of 100 g per batch. Accordingly, 100.000 g of uranium (as metal or hydride powder) was blended in a glass jar with 64.047 g of ammonium chloride, which was sufficient to react with 95% of the uranium in the feed materials. Then 49.566 g of alkali-metal chloride (i.e., sodium chloride or lithium chloride – potassium chloride eutectic) was blended with the uranium feed and ammonium chloride in the same jar. This dry blend was then transferred into a glassy carbon crucible, which was covered and heated to approximately 773 K at 10 K/hr to sublimate the ammonium chloride and thereby chlorinate the uranium metal or hydride. The lithium chloride – potassium chloride

mixtures were then heated to 923 K at 5 K/min to ensure molten conditions, while the sodium chloride mixtures were heated to 1123 K at 5 K/min for the same reason. The furnace cover was then removed, and each molten mixture was stirred momentarily with a glassy carbon rod to ensure homogeneity and visually verify the absence of any substantial solid phase. A ported cover was then placed atop the crucible, and the melt temperature was lowered to 773 K for the lithium chloride – potassium chloride mixtures and 923 K for the sodium chloride mixtures. A dip sample of the molten salt was taken with a glassy carbon rod, after which a uranium metal rod was suspended in the salt pool to a depth of approximately 1 cm. An electrolytic cell was established between the glassy carbon crucible as the anode and the uranium metal rod as the cathode to electrotransport excess uranium metal in contact with the crucible to the uranium metal rod at a controlled potential for an overnight period. The electrolytic cell was stopped, and the system was left at an open circuit for several hours. The uranium rod was removed, and a dip sample of the salt was taken with a glassy carbon rod. The furnace was de-energized, and the crucible was removed following sufficient cool down. Post-run components and products were weighed and transferred to sealed storage containers for future use. The series of four synthesis runs was performed with the lithium chloride – potassium chloride, ammonium chloride, uranium metal and uranium hydride powders first, followed by those with sodium chloride. A summary of conditions for this series of runs is shown in Table 1.

## 2.2 Equipment

A bench-top jeweler furnace (Kerr, Auto Electro-Melt Furnace, Maxi 3kg) was used to perform the series of synthesis runs. The furnace instrumentation was modified to facilitate ramp rate and cut-out temperature controls. The vendor-provided graphite crucible within the furnace was machined to accommodate a tapered glassy carbon crucible (SIGRADUR, GAT 32,

320 ml). The glassy carbon crucible was fitted with a glassy carbon cover (SIDRADUR, GAD 3), atop which steel wool was placed and around which a steel mesh ring was fitted. The nested crucibles, cover, steel wool and ring were covered with an insulated vendor-provided lid, as shown in Figure 1, which constituted the configuration of the furnace for initial heating of the salt mixtures. A separate ported furnace cover was fabricated to replace the vendor-provided lid to facilitate salt sampling and electrolytic cell operations. The various components utilized in the furnace during heat up and electrolytic cell operations are also shown in Figure 1. A 9-mm diameter by 250-mm long glassy carbon rod (SIGRADUR) was used for salt stirring and dip salt sampling.

An electrolytic cell was established in each molten salt pool during the series of synthesis runs by connecting electrical leads from a potentiostat (Solartron, model 1287) to a steel rod threaded into the graphite crucible (working electrode) and a uranium rod suspended in the salt pool (counter electrode) via an electrically insulated furnace cover port. A simplified diagram of the electrolytic cell is shown in Figure 2.

The furnace was positioned and operated inside an argon-atmosphere radiological glovebox (MBRAUN, LABmaster pro dp) located within Idaho National Laboratory (INL)'s Fuel Conditioning Facility. The glovebox was configured with a purification system that maintained oxygen and moisture concentrations in its atmosphere below 20 and 1 ppm, respectively. Sealed feedthroughs into the glovebox accommodated electrical leads for the furnace and potentiostat to support the described operations. Ammonia and hydrogen chloride gas detectors (Dräger diffusion tubes) were positioned directly above the furnace and at the opposite end of the glovebox during portions of the latter two synthesis runs.

### 2.3 Materials

The primary materials for this series of synthesis runs consisted of uranium feed materials, ammonium chloride, and alkali-metal halide salts, each requiring its own preparation. Specifically, the uranium metal powder was prepared by chopping a depleted uranium metal rod (Aerojet Ordnance Tennessee, Inc.) and alternately exposing up to 100 g of it at a time to a vacuum (~30 mTorr) and a pure hydrogen atmosphere (ambient pressure) at nominal 30-minute intervals in a sealed chamber within a horizontal tube furnace at 548 ± 25 K. The furnace was operated in an argon-atmosphere radiological glovebox at INL's Fuels and Applied Science Building. The glovebox was configured with a purification system that maintained oxygen and moisture concentrations in its atmosphere below 10 and 1 ppm, respectively. Exposure of the uranium metal to hydrogen gas at temperature promoted the formation of particulate uranium hydride via the following reaction and calculated Gibbs energy change. [6]

$$U + 3/2 H_2 (g) \rightarrow UH_3$$
  $\Delta G_{Rx,548K} = -25 \text{ kJ}$  (10)

Subsequent vacuum conditions promoted the reverse of Eq. 10 to form uranium metal powder. The uranium hydriding/dehydring cycle was repeated several times, after which the furnace was unloaded and the product transferred to a 50-mesh sieve. The uranium metal particles below 50-mesh were collected as feed material for uranium trichloride synthesis runs, while the particles above 50-mesh were reloaded into the furnace along with additional uranium metal pieces, as needed, for uranium metal powder formation. The production of uranium hydride was accomplished by loading 100.000 g of uranium metal powder (i.e., -50 mesh) in the furnace and heating the powder to  $548 \pm 25$  K under a pure hydrogen atmosphere for several hours. The chamber was then unloaded, and the uranium hydride powder was collected as feed material for

synthesis runs. Accordingly, 101.000 and 101.100 g of uranium hydride were prepared for synthesis runs 2 and 4.

Two uranium rods, one for contact with the lithium chloride – potassium chloride melts and the other for contact with the sodium chloride melts, were used as part of an electrolytic cell in this study. Each rod was cast from depleted uranium metal (Aerojet Ordnance Tennessee, Inc.) into 6-mm diameter by 150-mm long rods.

Ammonium chloride is hygroscopic and was unavailable in an anhydrous form from suppliers. Consequently, the ammonium chloride (Alfa Aesar, 99.999%, Puratronic) used in this study was dried and sieved to the desired particle size using a bench-top box furnace in an argonatmosphere glovebox. Specifically, the procured granular ammonium chloride was loaded into trays and heated to 393 K for at least 20 hours, followed by heating at 413 K for at least four hours. The dried material was crushed and sieved to particle sizes below 30-mesh.

Lithium chloride – potassium chloride eutectic (Sigma Aldrich, 99.99%, 44 wt% LiCl) and sodium chloride (Sigma Aldrich, 99.999%) were procured as anhydrous -10 mesh beads packaged under argon. Each of these alkali-metal chlorides was crushed and sieved to particle sizes below 30-mesh.

### 2.4 Sample Characterization

Salt samples from the series of synthesis runs, including one before and one after each electrolytic cell conditioning operation for a set of eight samples, were split into additional sample sets and subjected to chemical, diffractometry, and microscopic analyses as follows. One set of eight synthesized salt samples was characterized for elemental makeup via inductively coupled plasma – optical emission spectroscopy (ICP-OES). Another set of eight synthesized

salt samples was characterized for chemical speciation via X-ray diffraction (XRD). Additional samples of feedstock lithium chloride – potassium chloride eutectic salt and previously synthesized lithium chloride – potassium chloride (eutectic) – uranium trichloride salt (containing 53 wt% U) from the aforementioned chlorine – cadmium chloride route by ANL researchers [5] were also characterized by XRD. The XRD sample analysis involved grinding each sample into a fine powder, loading it onto a tray, and sealing it with a domed cover under a dry argon atmosphere to preclude moisture absorption into the sample. Each covered sample was analyzed with a PANalytical AERIS X-ray diffractometer (Malvern Panalytical, LLC), equipped with a Cu K $\alpha$  source at 40 kV and 15 mA. Scan parameters were  $10-110^{\circ}$  with a step of  $0.0109^{\circ}$  and a counting time of 118 s.

The latter set of eight salt samples was also characterized with a Titan Themis 200 probe Cs corrected extreme field emission gun (X-FEG) scanning transmission electron microscope (STEM), which provided sub-angstrom imaging and spectroscopy. The microscope was equipped with a super-x energy-dispersive X-ray spectroscopy (EDS) system and a Gatan Continuum system.

### 3. Calculations

The high-surface area of uranium metal and uranium hydride feed materials, along with the multiple constituent phases that were expected in this series of runs, created a complex set of conditions that warranted calculations prior to proceeding with the experiments. Specifically, a model was created to assess possible chemical equilibrium conditions and related reaction mechanisms to ensure that uranium trichloride would be produced in the respective media. Additionally, a conservative adiabatic reaction temperature determination was conducted to

ensure that a worst-case exotherm in a synthesis run was manageable using the described experimental conditions and equipment configurations.

Chemical equilibrium calculations provide a straightforward means of assessing product compositions as a function of temperature for a given quantity of raw materials. Commercially available software, HSC Chemistry 8, [6] was used to perform such calculations with a Gibbs energy minimization model, which was based on prior work by others. [16] After inputting the defined feed materials for synthesis run 1 and assuming unit activities and ideal mixing, the model produced a plot of possible constituent concentrations as a function of temperature (see Figure 3). Only the predominant compounds of over 30 selected possible compounds are shown in Figure 3. Noteworthy findings from the model are (1) the predominant formation of uranium trichloride compared to an inconsequential amount of uranium tetrachloride and (2) the decomposition of ammonia into nitrogen and hydrogen gases from possible intermediate reactions with uranium metal. The latter finding suggests overall reactions for uranium trichloride synthesis per the following reactions and calculated Gibbs energy in lieu of, or in addition to, those in Eqs. 8 and 9.

$$U + 3 NH_4Cl \rightarrow UCl_3 + 3/2 N_2(g) + 6 H_2(g)$$
  $\Delta G_{Rx,611K} = -467 kJ$  (11)

$$UH_3 + 3 NH_4Cl \rightarrow UCl_3 + 3/2 N_2(g) + 15/2 H_2(g)$$
  $\Delta G_{Rx,611K} = -454 kJ$  (12)

A similar model was created for synthesis run 2, which produced a nearly identical outcome, apart from a higher hydrogen concentration owing to the decomposition of uranium hydride. Additional models were generated for synthesis runs 3 and 4, which produced similar outcomes to those from runs 1 and 2, aside from the unchanging presence of sodium chloride in lieu of lithium and potassium chloride.

Uranium metal and uranium hydride powders are pyrophoric materials, as they can ignite and rapidly burn in air in an uncontrolled manner. Consequently, these powders were prepared and handled under inert argon atmospheres in this study. However, this study pursued blending of a hydrogen chloride source, in the form of sublimating ammonium chloride, together with a near stoichiometric mass of uranium metal or uranium hydride powder, as opposed to metering one reactive component into the other. Thus, an adiabatic reaction temperature determination was performed per the following energy balance to assess the consequences of an accelerated reaction per Eq. 8, which represents runs 1 and 3 with a worse case exothermic heat of reaction  $(\Delta H_{Rx})$  at -86 kJ, as compared to +48 kJ for runs 2 and 4 per Eq. 9. [6]

$$\Delta H_{Rx} = \int_{T_i}^{T_f} \sum n_i * C_{p,i} (T) * dT$$
 (13)

where:  $T_i = initial temperature$ 

 $T_f$  = final temperature

 $n_i$  = stoichiometric moles of reaction product i

 $C_{pi}$  = heat capacity of reaction product i

In this calculation, it was conservatively assumed that no reaction occurred during the heating of a mixture from run 1 or 3 until the sublimation point of ammonium chloride (611 K) was reached, at which point the heat of reaction was fully absorbed by the reaction products alone. Accordingly, the initial temperature used in Eq. 13 was 611 K. Given heat capacities as a function of temperature for the reaction products, [6] the final temperature (i.e., adiabatic reaction temperature) per Eq. 13 was determined to be 903 K. Thus, an accelerated reaction per Eq. 8 was deemed sufficiently bounded by the experimental conditions and test configuration, as the adiabatic reaction temperature was below the planned operating temperatures of 923 and 1123 K for runs 1 and 3, respectively.

### 4. Results

The prescribed uranium metal powder, ammonium chloride, and lithium chloride – potassium chloride eutectic salts were blended in a 250-ml glass jar, as shown in Figure 4, for uranium trichloride synthesis run 1. The mixture was transferred to a pre-weighed glassy carbon crucible, also shown in Figure 4. After heating the mixture to 923 K, the furnace lid was removed, and no discoloration of the steel wool or mesh was observed. The molten solution was stirred, and no substantial solid phase was apparent. Molten salt dip samples were taken, as shown in Figure 5, both before (sample A) and after (sample B) the described electrolytic cell operations. The uranium metal rod exhibited a net mass loss of 2.518 g, despite an applied charge of 3237 C at a controlled cell voltage of 1V that produced a variable current between 25 and 75 mA over a period of nearly 16 hours. The furnace was de-energized, and the cooled salt ingot separated readily from the glassy carbon crucible. The ingot was dark, as shown in Figure 5, with an apparent density of 3.4 g/cc based on mass and gross dimensions.

The procedure was repeated for uranium trichloride synthesis runs 2-4, as outlined in Table 1. No discoloration or notable increase in mass was observed on the steel wool or ring throughout the runs, nor was any substantial solid phase detected prior to electrolytic cell operations. Each product salt ingot from runs 1-4 was similar in appearance and size. No degradation or notable change in mass was observed in the glassy carbon crucible throughout the series of runs. Mass measurements for each run are listed in Table 2. Small decreases in mass were observed in the respective uranium metal rods for runs 1, 3, and 4, while a slight increase in mass was observed on the rod for run 2.

For run 3, ammonia gas detection tubes were positioned directly above the furnace (near) and at the opposite end of the glovebox (far). The near and far tubes read 500 and 200 ppm,

respectively, after 25 hours of run time with the furnace at 553 K, while the same tubes read 1500 (maximum reading) and 800 ppm, respectively, after 47 hours of run time with the furnace at 773 K.

For run 4, both ammonia and hydrogen chloride gas detections tubes were positioned in pairs near and far from the furnace. The near and far ammonium gas detection tubes read 1300 and 700 ppm, respectively, after 22 hours of run time with the furnace at 523 K, while the same tubes read 1500 (maximum reading) and 800 ppm, respectively, after 27 hours of run time with the furnace at 573 K. The near ammonium gas detection tube remained at 1500 ppm after 47 hours of run time with the furnace at 773 K, while the far tube read 1100 ppm. Neither hydrogen chloride gas detection tube indicated a presence of the gas during run 4.

Each of the eight salt samples from runs 1-4 was split roughly in half for post-run characterization. The first set of samples was analyzed for primary elements via ICP-OES. The results with a margin of error of  $\pm$  5% at 2 sigma are shown in Table 3.

The second set of eight samples were ground to a powder in an argon-atmosphere glovebox for XRD and STEM analyses. Samples of the feedstock LiCl-KCl and ANL-synthesized LiCl-KCl-UCl<sub>3</sub> were similarly prepared and analyzed via XRD to compare results with those from the synthesized uranium salts in this study. The XRD patterns of salt samples from runs 1 and 2 in LiCl-KCl are shown in Figures 6. The XRD patterns for the feedstock LiCl-KCl and ANL-synthesized salt samples are shown together with that from sample 2B in Figure 7, while XRD patterns for salt samples from runs 3 and 4 in NaCl are shown in Figure 8. STEM images of samples 1A, 2A, 3A, and 4A are shown in Figure 9, while those for samples 1B, 2B, 3B, and 4B are shown in Figure 10. Compositions of the samples from runs 1 – 4, based

on EDS from images in Figures 9 and 10, are listed in Table 4. A STEM-EDS map of sample 1A is shown in Figure 11.

### 5. Discussion

The theoretical compositions of reaction products per Eqs. 8 and 9 for the series of uranium trichloride synthesis runs were calculated based on the feed material input and the following assumptions. First, the prescribed blends of uranium feed material, ammonium chloride, and alkali-metal halide in the glass jar did not all transfer to the glassy carbon crucible, as some residual powder adhered to the inner jar walls. It was assumed that the mixtures, transferred to the glassy carbon crucible for each run, contained the same proportions of materials that were initially loaded in the respective glass jars. Second, all the nitrogen and hydrogen from ammonium chloride and uranium hydride, as applicable, separated from the reaction product as an off-gas. Third, all the chloride from ammonium chloride was retained in the reaction to form uranium trichloride in the molten phase. Fourth, excess uranium metal, including the net mass gain or loss from the uranium metal electrode, was ascribed to an insoluble metal phase. Finally, the alkali-metal chlorides were present entirely in the molten phase without any reaction or material loss. Accordingly, the calculated elemental compositions of reaction product phases from the series of synthesis runs are shown in Table 5.

The performance of the series of synthesis runs can be assessed by comparing the calculated and measured composition values. Specifically, the combination of the measured salt sample and salt ingot masses for each run from Table 2 can be compared to the corresponding calculated total salt product mass from Table 5 to assess an overall material balance, as shown in Table 6.

The overall material balances exhibited excellent consistencies between the measured and calculated values for each of the synthesis runs, supporting the assumption that essentially all the nitrogen and hydrogen from the ammonium chloride and uranium hydride, as applicable, separated from the salt product while all the chloride remained behind. This observation was also substantiated by the presence of ammonia gas in the glovebox during the latter two runs and the absence of hydrogen chloride gas detection in the last run.

The calculated elemental concentrations can also be determined and compared to measured values to further assess performance of the series of runs. Specifically, the calculated uranium, potassium, lithium, and sodium concentrations in the molten phase (see Table 5) are compared to the measured values (see Table 3), including ratios of uranium to other metal cations, as shown in Table 7.

The calculated and measured concentrations of uranium, potassium, and lithium in runs 1 and 2 were relatively consistent, excepting slightly higher measured potassium and lithium values for run 2. The ratios of uranium concentrations to the respective alkali-metal concentrations provided a check on possible analytical error, in the case that all constituents for a particular sample were consistently high or low. While the calculated and measured ratios for run 1 were relatively consistent, those for run 2 were generally low. Thus, it appeared that conversion of uranium hydride to uranium trichloride in run 2 was lower than that in run 1. A favorable overall material balance (including chlorine inventory) for run 2 and a lower apparent trichloride concentration might suggest that some uranium tetrachloride formed and did not convert to uranium trichloride per Eq. 7.

The measured uranium and sodium concentrations in runs 3 and 4 were consistently lower than the calculated values. However, the measured uranium to sodium concentration ratio

was nearly identically to the calculated value for run 4, while that for run 3 was slightly lower. Thus, it appeared that uranium hydride facilitated a higher conversion to uranium trichloride in run 4 than that of uranium metal in run 3. Again, the favorable material balances and lower apparent trichloride concentration in run 3 could suggest the presence of a minor fraction of uranium tetrachloride.

The initial heat-up rate for the series of synthesis runs was intentionally set at a low rate of 10 K/hr to meter the gasification and consequent delivery of hydrogen chloride reactant into the reactive, high-surface area uranium feed materials. The low heat-up rate also served to promote residence time for gaseous hydrogen chloride to react with the uranium feed materials. The parity between calculated and measured material balances for the series of synthesis runs suggests that no appreciable unreacted hydrogen chloride escaped from the glassy carbon crucible, which is further substantiated by the absence of steel wool or ring degradation and the lack of hydrogen chloride detection in gaseous diffusion tubes. On the other hand, gaseous ammonia was routinely observed during the runs in which the respective gaseous diffusion tubes were installed, suggesting that uranium trichloride synthesis occurred, at least in part, by the reactions identified in Eqs. 8 and 9.

The intent of applying an electrolytic cell to the synthesized molten salt was to remove excess uranium metal from the product. The applied cell voltage provided ample overpotential to oxidize uranium metal in contact with the glassy carbon crucible without oxidizing uranium (III) ions to uranium (IV) ions. [17] However, in runs 1, 3, and 4, uranium metal was added to the system instead of being removed. It is possible that uranium deposits on the cathode rod in runs 1, 3, and 4 along with some uranium from the rod itself dislodged and dropped back into the salt pool during the open circuit period at the end of each run. It is also possible that the uranium

metal rod reacted with residual uranium tetrachloride in the salt to form uranium trichloride per Eq. 7, despite the initial loading of excess uranium as metal or hydride. Although the electrolytic cell failed to remove excess uranium in most of the synthesis runs, it did promote increased ratios of uranium to alkali-metal concentrations in the salt for runs 1, 2 and 3, while those for run 4 were very near the calculated value. If separation of excess uranium metal from the synthesized salt were necessary, then vacuum distillation of the salt could be performed; however, such was beyond the scope of this study.

The XRD patterns of sample material from runs 1 and 2 (see Figure 6) exhibited a significant number of peaks of varying intensities, reflecting a number of possible species in the salt samples. The patterns from samples 1A, 1B, and 2B were reasonably consistent, while that from sample 2A was less consistent and exhibited lower peak intensities. The reactions of ammonium chloride with excess uranium metal and hydride per Eqs. 8 and 9 were expected to produce uranium trichloride. However, the formation of uranium tetrachloride was possible in the absence of localized excess uranium metal or hydride. The combination of lithium chloride, potassium chloride, uranium trichloride, and uranium tetrachloride could have led to several mixed chloride formations, e.g., K<sub>2</sub>UCl<sub>5</sub>, K<sub>2</sub>UCl<sub>6</sub>, and Li<sub>2</sub>UCl<sub>6</sub>, as identified in their respective binary phase diagrams. [18-19] However, only LiCl (lattice parameters a = 5.138 Å, b = 5.138 Å,  $c = 5.138 \text{ Å}, \alpha = 90^{\circ}, \beta = 90^{\circ}, \gamma = 90^{\circ}), KCl (a = 6.288 \text{ Å}, b = 6.288 \text{ Å}, c = 6.288 \text{ Å}, \alpha = 90^{\circ}, \beta = 90^{\circ},$  $90^{\circ}$ ,  $\gamma = 90^{\circ}$ ), UCl<sub>3</sub> (a = 7.444 Å, b = 7.444 Å, c = 4.324 Å,  $\alpha = 90^{\circ}$ ,  $\beta = 90^{\circ}$ ,  $\gamma = 120^{\circ}$ ), and  $K_2UCl_5$  (a = 12.722 Å, b = 8.806 Å, c = 7.995 Å,  $\alpha$  = 90°,  $\beta$  = 90°,  $\gamma$  = 90°) were definitively identified in the XRD patterns for runs 1 and 2. Predominant peaks (e.g., 22.6, 33.7, 39.8, and 41.0 degrees 2θ) in the XRD patterns for runs 1 and 2 were unidentified, which could be attributed to other mixed chloride species not identified in the referenced phase diagrams.

Interestingly, the XRD pattern for ANL-synthesized LiCl-KCl-UCl<sub>3</sub> (see Figure 7), which was not expected to contain tetravalent uranium from its synthesis route, exhibited a similar pattern to those for runs 1 and 2, including the predominant unidentified peaks from the patterns in Figure 6. The XRD pattern for the feedstock LiCl-KCl eutectic salt (see Figure 7) exhibited a substantially smaller set of peaks, which were consistent with those for runs 1 and 2 in Figure 6. In short, the confirmed presence of uranium trichloride, as UCl<sub>3</sub> and K<sub>2</sub>UCl<sub>5</sub>, in the XRD patterns for runs 1 and 2, the similarity of the ANL-synthesized LiCl-KCl-UCl<sub>3</sub> pattern to those for runs 1 and 2, and the relatively high uranium concentrations in the salt samples from runs 1 and 2 (see Table 7) all suggest that the synthesized salt products for runs 1 and 2 predominantly contained trivalent uranium. However, the presence of tetravalent uranium in these samples could not be conclusively dismissed, given some predominant unidentified peaks in the respective patterns.

The XRD patterns of sample material from runs 3 and 4 (see Figure 8) were remarkably consistent between each sample, and they contained fewer peaks than those in runs 1 and 2. The primary expected constituents in runs 3 and 4 were sodium chloride and uranium trichloride, both of which were identified in the respective XRD patterns. The phase diagram for sodium chloride and uranium trichloride [14] does not identify a mixed chloride. No uranium tetrachloride or mixed sodium chloride and uranium tetrachloride (e.g., Na<sub>2</sub>UCl<sub>6</sub>) were identified in these patterns. It should be noted that all of the XRD patterns in this study exhibited a broad rounded amorphous peak near 17 degrees 2θ, which was an artifact of the polymeric dome cover on the XRD sample plates.

The STEM images in Figures 9 and 10 exhibited a variety of crystalline structures. Dark needle-like structures were observed in samples 1A and 4A, while dark spots were apparent in

samples 1B, 2B, and 4B. Dark planar structures were observed in samples 2A, 3A, and 3B. Generally, the images of samples before electrolytic conditioning (see Figure 9) appeared to be more heterogeneous with sharper edges, while those after electrolytic conditioning (see Figure 10) appeared to be more homogeneous with smoother surfaces.

The EDS composition of samples from runs 1-4 (see Table 4) exhibited relatively wide ranges of constituent concentrations, denoting a likely heterogeneity of examination points within the samples, whereas the elemental analysis results (see Table 3) defined the respective contents of entire samples. It should also be noted that the sample results from runs 1 and 2 excluded lithium, due to the inability of EDS to detect this light element. Discounting lithium, the calculated values for uranium, chlorine, and potassium in runs 1 and 2 were 14, 73, and 13 at%, respectively, while those from EDS ranged respectively from 40-49 at%, 39-51 at%, and 7-21 at%. Thus, EDS exhibited a higher-than-expected presence of uranium in the run 1 and 2 samples. The calculated values for uranium, chlorine, and sodium in runs 3 and 4 were 12, 62, and 26 at%, respectively, while those from EDS ranged respectively from 20-39 at%, 45-57 at%, and 14-27 at%. Similarly, the EDS exhibited a predominant presence of uranium in the run 3 and 4 samples.

The STEM-EDS map of sample 1A in Figure 11 identified a uranium concentration density map that was consistent with the dark needle-like crystalline structures. Furthermore, the potassium concentration density map was consistent with that of uranium, suggesting a possible mixed potassium and uranium chloride phase (e.g., K<sub>2</sub>UCl<sub>5</sub>) like that observed in the XRD patterns for this same sample (see Figure 6).

### 6. Conclusions

A series of four experiments was successfully conducted, producing uranium trichloride from uranium metal or uranium hydride powder and ammonium chloride in either a lithium chloride – potassium chloride eutectic or sodium chloride medium. Near stoichiometric blends of uranium and ammonium chloride particulate along with select alkali-metal chloride particulate were heated at a low initial heat-up rate of 10 K/hr. The low heat-up rate effectively metered hydrogen chloride to react with the high-surface area uranium metal or hydride. This approach provided sufficient residence time for chlorination of uranium and its consequent fusion with the respective alkali-metal chlorides without any notable loss of chlorine from the system, based on material balances and hydrogen chloride detection mechanisms during the series of runs.

Nitrogen and hydrogen from the ammonium chloride and uranium hydride feed materials were liberated in the reaction, dissipating in gaseous diatomic and ammonia forms. The products from the series of runs were dark consolidated salt ingots with an apparent density of 3.4 g/cc.

Chemical analysis of molten samples from each salt product revealed uranium concentrations ranging from 44 – 51 wt% compared to an expected concentration of 50.8%; however, uranium to alkali metal concentration ratios were closer to expected values. Characterization of ternary salt product samples from runs 1 and 2 via XRD definitively identified the presence of LiCl, KCl, UCl<sub>3</sub> and K<sub>2</sub>UCl<sub>5</sub>; however, several prominent peaks in the XRD patterns could not be identified. Consequently, the presence of uranium tetrachloride could not be conclusively dismissed, despite constituent concentrations and ratios from chemical analysis that suggested otherwise. Diffractometry of binary salt product samples from runs 3 and 4 only identified sodium chloride and uranium trichloride. No uranium tetrachloride in simple or mixed form was identified in the binary salt product samples. Microscopic analyses of product

samples identified needle-like and planar crystalline structures, while EDS mapping identified broad constituent compositions and revealed higher-than-expected uranium concentrations.

Efforts are underway to speciate trivalent and tetravalent uranium in the synthesized salt samples using STEM-Electron Energy Loss Spectroscopy, which will be reported separately.

### Acknowledgements

This work was supported by Idaho National Laboratory's Laboratory Directed Research and Development program under the U.S. Department of Energy (DOE), Office of Nuclear Energy, Idaho Operations Office under contract DE-AC07-05ID14517.

### References

- [1] U.S. Department of Energy. 2000. "Record of Decision for the Treatment and Management of Sodium-Bonded Spent Nuclear Fuel." Federal Register 65, no. 182.
- [2] U.S. Department of Energy. 2000. "Final Environmental Impact Statement for the Treatment and Management of Sodium-Bonded Spent Nuclear Fuel." DOE/EIS-0306.
- [3] National Research Council. 2000. *Electrometallurgical Techniques for DOE Spent Fuel Treatment: Final Report*. Washington D.C.: National Academy Press.
- [4] U.S. Department of Energy. 2016. "Energy Department Announces New Investments in Advanced Nuclear Power Reactors to Help Meet America's Carbon Emission Reduction Goal." Accessed March 16, 2021. https://www.energy.gov/articles/energy-department-announces-new-investments-advanced-nuclear-power-reactors-help-meet.

- [5] W. E. Miller and Z. Tomczuk. 2004. Method for Making a Uranium Chloride Salt Product. US Patent 6,800,262.
- [6] Outotec, HSC Chemistry 8, Pori (2015).
- [7] B. R. Westphal, J. C. Price, R. D. Marini. 2011. "Synthesis of Uranium Trichloride for the Pyrometallurgical Processing of Used Nuclear Fuel." Fray International Symposium on Molten Salts and Ionic Liquids 2011. Accessed March 17, 2021. http://www.inl.gov/technicalpublications/Documents/5415161.pdf.
- [8] H. Lambert, T. Kerry, C. A. Sharrad. 2018. "Preparation of Uranium (III) in a Molten Chloride Salt: A Redox Mechanistic Study." Journal of Radioanalytical and Nuclear Chemistry 317, 925–932. https://doi.org/10.1007/s10967-018-5953-7.
- [9] G. Y. Kim, T. J. Kim, J. Jang, H. C. Eun, S. J. Lee. 2018. "Synthesis of Uranium Trichloride Salt Using ZnCl<sub>2</sub>." Journal of Radioanalytical and Nuclear Chemistry 318, 2173–2176. http://doi.org/10.1007/s10967-018-6134-4.
- [10] P. Souček, R. Malmbeck, E. Mendes, C. Nourry, R. Jardin, J.-P. Glatz. 2009. "Separation of Uranium from Uranium-Aluminum Alloys by Chlorination Process," Global 2009, 1214-1220.
- [11] R. Meier, P. Souček, R. Malmbeck, T. Fanghänel. 2012. "Recycling of Uranium from Uranium-Aluminum Alloys by Chlorination with HCl(g)," Procedia Chemistry 7, 785-790.

- [12] H. C. Eun, T. J. Kim, J. H. Jang, G. Y. Kim, S. J. Lee, J. M. Hur. 2017. "A Study of Chlorination of Uranium Metal Using Ammonium Chloride." Journal of Radioanalytical Nuclear Chemistry 314, 533–537. https://doi.org/10.1007/s10967-017-5359-y.
- [13] A. L Hames, A. Paulenova, J. L. Willit, M. A. Williamson. 2018. "Phase Equilibria Studies of the LiCl-KCl-UCl<sub>3</sub> System." Nuclear Technology 203, 272–281. https://doi.org/10.1080/00295450.2018.1448673.
- [14] C. A. Kraus, "System NaCl-UCl<sub>3</sub>," (1959) Phase Equilibrium Diagram 1318 in *ACerS NIST Phase Equilibria Diagrams*, National Institute of Standards and Technology, PC Database, Version 4.0, Gaithersburg, Maryland (2013).
- [15] S. Ghosh, B. P. Reddy, K. Nagarajan, K. C. H. Kumar. 2014. "Experimental Investigations and Thermodynamic Modeling of KCl-LiCl-UCl<sub>3</sub> System." CALPHAD: Computer Coupling of Phase Diagrams and Thermochemistry 45 (June): 11-26. https://doi.org/10.1016/j.calphad.2013.11.001.
- [16] W. B. White, S. M. Johnson, G. B. Dantzig. 1958. "Chemical Equilibrium in Complex Mixtures." The Journal of Chemical Physics 28 (751). https://doi.org/10.1063/1.1744264.
- [17] J. A. Plambeck. 1976. "Fused Salt Systems." In Encyclopedia of Electrochemistry of the Elements, Vol. X, edited by A. J. Bard, New York: Marcel Dekker, Inc.
- [18] I. G. Suglobova and D. E. Chirkst, "System KCl-UCl<sub>3</sub>," (1981) Phase Equilibrium Diagram 93-275 in ACerS – NIST Phase Equilibria Diagrams, National Institute of Standards and Technology, PC Database, Version 4.0, Gaithersburg, Maryland (2013).

[19] C. J. Barton, A. B. Wilkerson, T. N. McVay, R. J. Sheil, and W. R. Grimes, "System KCl-UCl<sub>4</sub>," (1959) Phase Equilibrium Diagram 1282 in *ACerS – NIST Phase Equilibria Diagrams*, National Institute of Standards and Technology, PC Database, Version 4.0, Gaithersburg, Maryland (2013).

Table 1. Conditions for series of uranium trichloride synthesis runs.

Run	Mixture	Mixture Heating			
1	U metal, NH <sub>4</sub> Cl, LiCl-				
1	KCl eutectic	Ambient $\rightarrow$ 773 K at 10 K/hr	1 V cell voltage at 773 K		
2	UH <sub>3</sub> , NH <sub>4</sub> Cl, LiCl-KCl	773 K $\rightarrow$ 923 K at 5 K/min	1 v con voitage at v v 11		
2	eutectic				
3	U metal, NH <sub>4</sub> Cl, NaCl	Ambient $\rightarrow$ 773 K at 10 K/hr	0.9 V cell voltage at 923 K		
4	UH <sub>3</sub> , NH <sub>4</sub> Cl, NaCl	773 K $\rightarrow$ 1123 K at 5 K/min	0.9 v cen voltage at 923 K		

Table 2. Summary of recorded masses from uranium trichloride synthesis runs 1-4.

grams	Run 1	Run 2	Run 3	Run 4
Mixture in crucible	213.493	214.484	213.488	214.645
Salt sample A	1.512	2.207	0.574	0.720
Salt sample B	1.192	1.112	0.907	1.341
Change in uranium rod	-2.518	+0.033	-2.252	-2.926
Salt ingot	192.505	188.996	191.836	192.766

Table 3. Salt sample elemental analysis results from ICP-OES.

ppm	Run 1		Run 2		Ru	n 3	Run 4		
Sample	A	A B		В	A	В	A	В	
U	513,000	508,000	506,000	484,000	441,000	458,000	451,000	447,000	
K	78,700	74,500	83,000	79,000					
Li	20,000	18,900	21,100	19,600					
Na					97,500	95,900	92,500	92,200	

Table 4. EDS compositions of samples from runs 1-4.

Samples	U		(	Cl		K	Na		
Z marpara	at%	wt%	at%	wt%	at%	wt%	at%	wt%	
1A	41.6	82.6	51.3	15.1	7.1	2.3	-	-	
1B	39.9	81.2	39.1	11.8	20.9	7.0	-	-	
2A	44.0	83.7	40.2	11.4	15.7	4.9	-	-	
2B	49.0	86.4	42.9	11.3	8.1	2.3	-	-	
3A	29.2	74.8	57.1	21.8	-	-	13.7	3.4	
3B	20.3	66.1	52.4	25.4	-	-	27.3	8.6	
4A	26.4	73.4	47.5	19.6	-	-	26.1	7.0	
4B	38.6	82.3	45.0	14.3	-	-	16.4	3.4	

Table 5. Calculated elemental composition of reaction product phases from runs 1-4.

grams	Run 1	Run 2	Run 3	Run 4						
Molten phase										
U	94.947	94.944	94.945	94.971						
K	14.549	14.548								
Li	3.569	3.569								
Na			19.487	19.493						
Cl	73.846	73.843	72.476	72.496						
Total molten phase	186.911	186.904	186.908	186.960						
Insoluble phase										
U	7.515	4.963	7.248	7.924						
Total salt product	194.426	191.867	194.156	194.884						
Gas phase										
N	16.761	16.761	16.761	16.765						
Н	4.825	5.824	4.825	5.926						
Total off gas	21.586	22.585	21.586	22.691						

Table 6. Comparison of overall material balance for series of synthesis runs.

	Run 1	Run 2	Run 3	Run 4
Measured salt product	195.209 g	192.315 g	193.317 g	194.827 g
Calculate salt product	194.426 g	191.867 g	194.156 g	194.884 g
-				
Measured : calculated salt product	100.4%	100.2%	99.6%	100.0%

Table 7. Comparison of calculated and measured constituent concentrations from series of runs.

wt%	Run 1		Run 2		Run 3			Run 4				
	Measi Calc.		Measured		Meas	Measured		Measured		Calc.	Measured	
sample		1A	1B		2A	2B		3A	3B		4A	4B
[U]	50.8	51.3	50.8	50.8	50.6	48.4	50.8	44.1	45.8	50.8	45.1	44.7
[K]	7.78	7.87	7.45	7.78	8.30	7.90						
[Li]	1.91	2.00	1.89	1.91	2.11	1.96						
[Na]							10.43	9.75	9.59	10.43	9.25	9.22
[U]:[K]	6.53	6.52	6.82	6.53	6.10	6.13						
[U]:[Li]	26.6	25.7	26.9	26.6	24.0	24.7						
[U]:[Na]							4.87	4.52	4.76	4.87	4.88	4.85



Figure 1. Furnace and components for synthesis runs, including heat-up configuration (left), disassembled components (center), and electrolytic cell configuration (right).

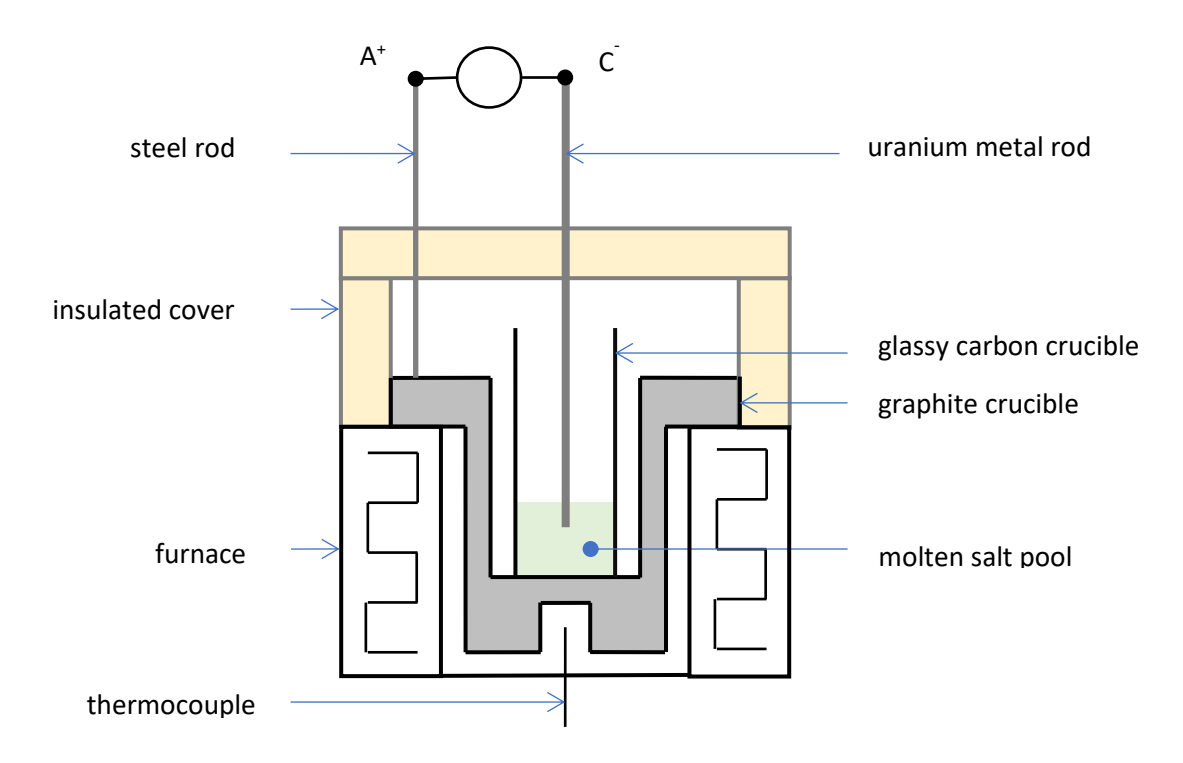


Figure 2. Simplified diagram of electrolytic cell for synthesis runs.

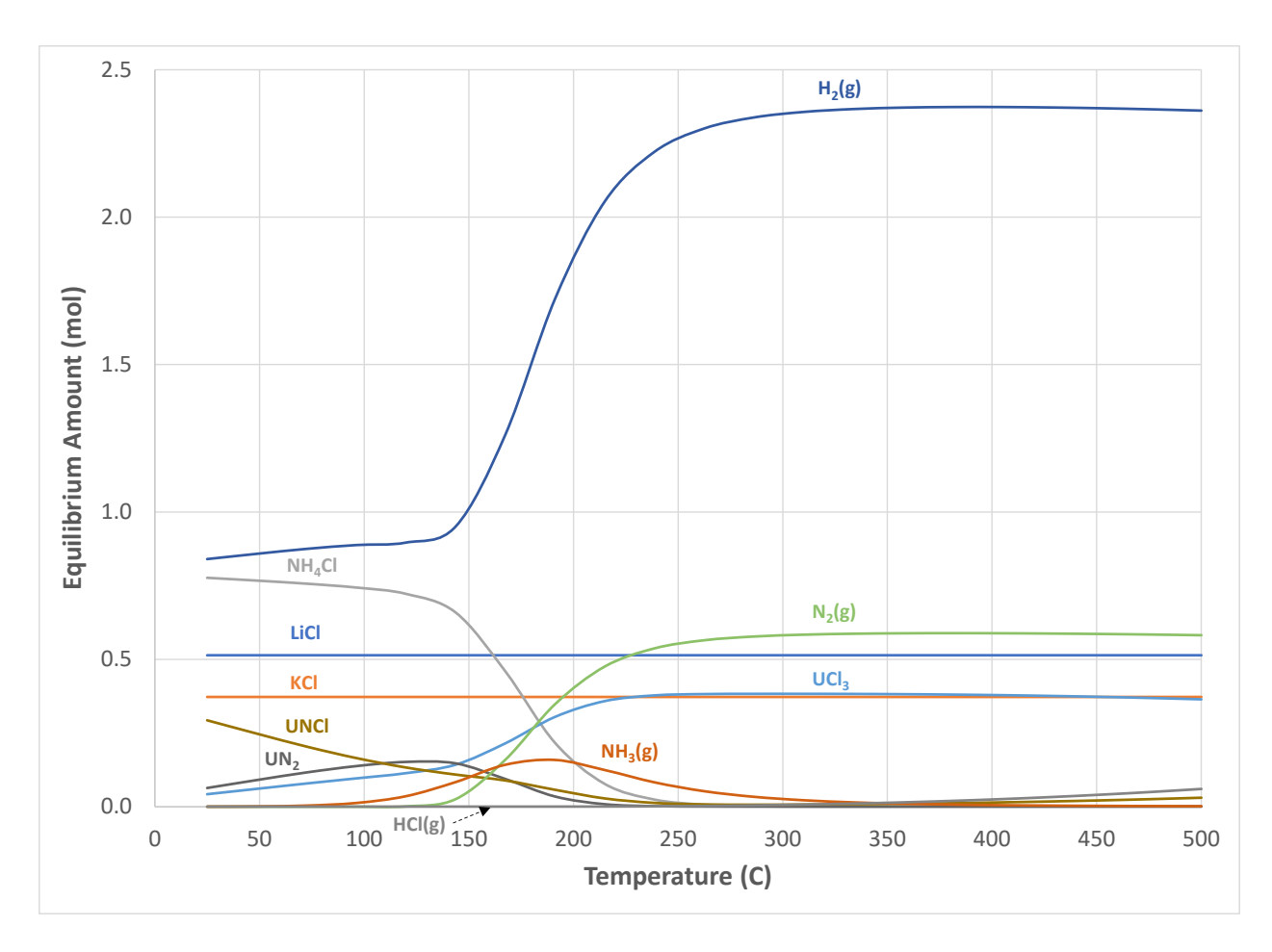


Figure 3. Modeled equilibrium constituent concentrations versus temperature for synthesis run 1.



Figure 4. Uranium metal powder, ammonium chloride, and lithium chloride – potassium chloride blend before (left) and after (right) loading in glassy carbon crucible.



Figure 5. Dip sample of molten salt after electrolytic cell operations in synthesis run 1 (left) and post-run salt ingot (right).

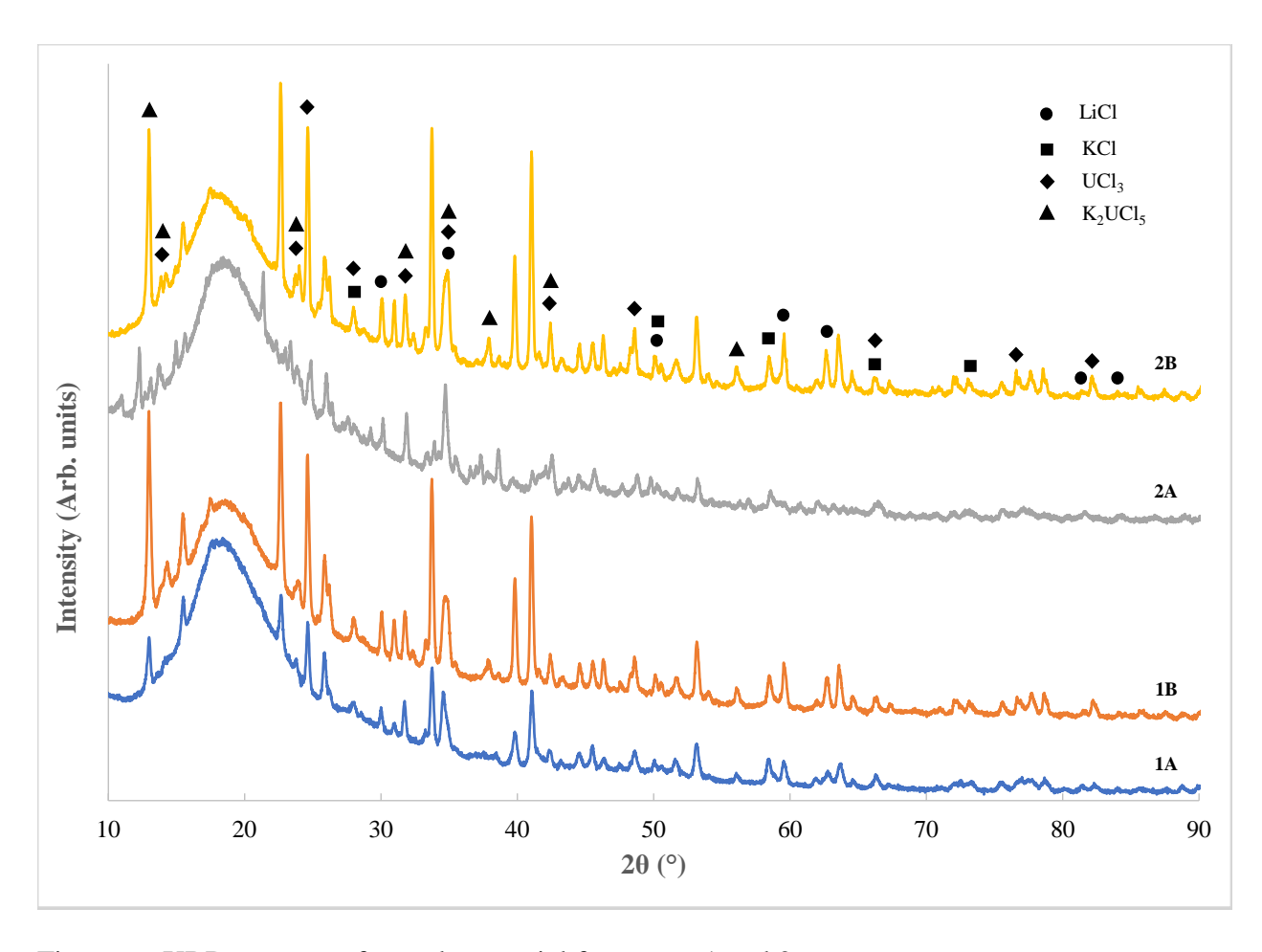


Figure 6. XRD patterns of sample material from runs 1 and 2.

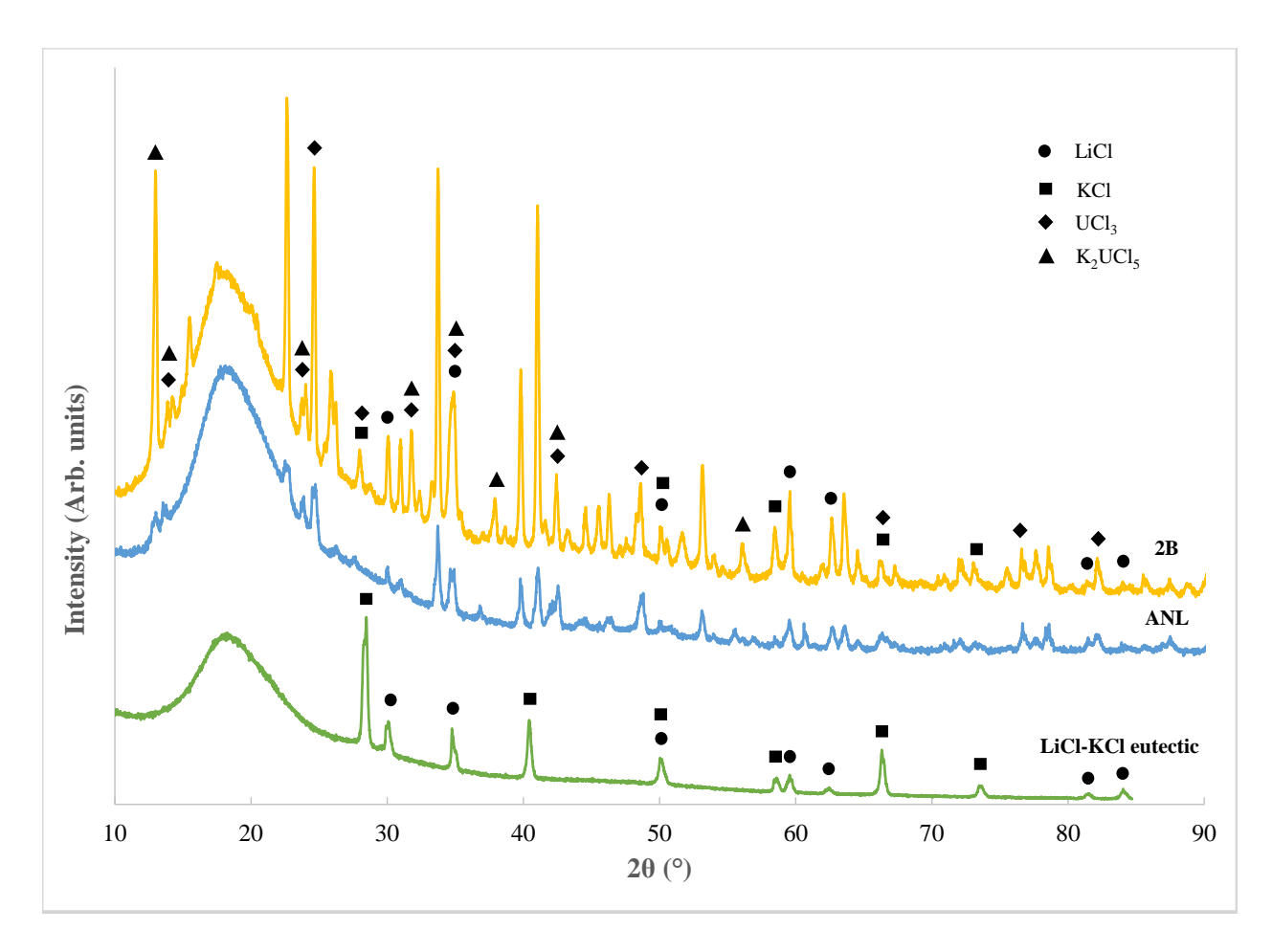


Figure 7. XRD patterns of feedstock LiCl-KCl eutectic and ANL-synthesized LiCl-KCl (eutectic)-UCl<sub>3</sub> sample material along with salt sample 2B.

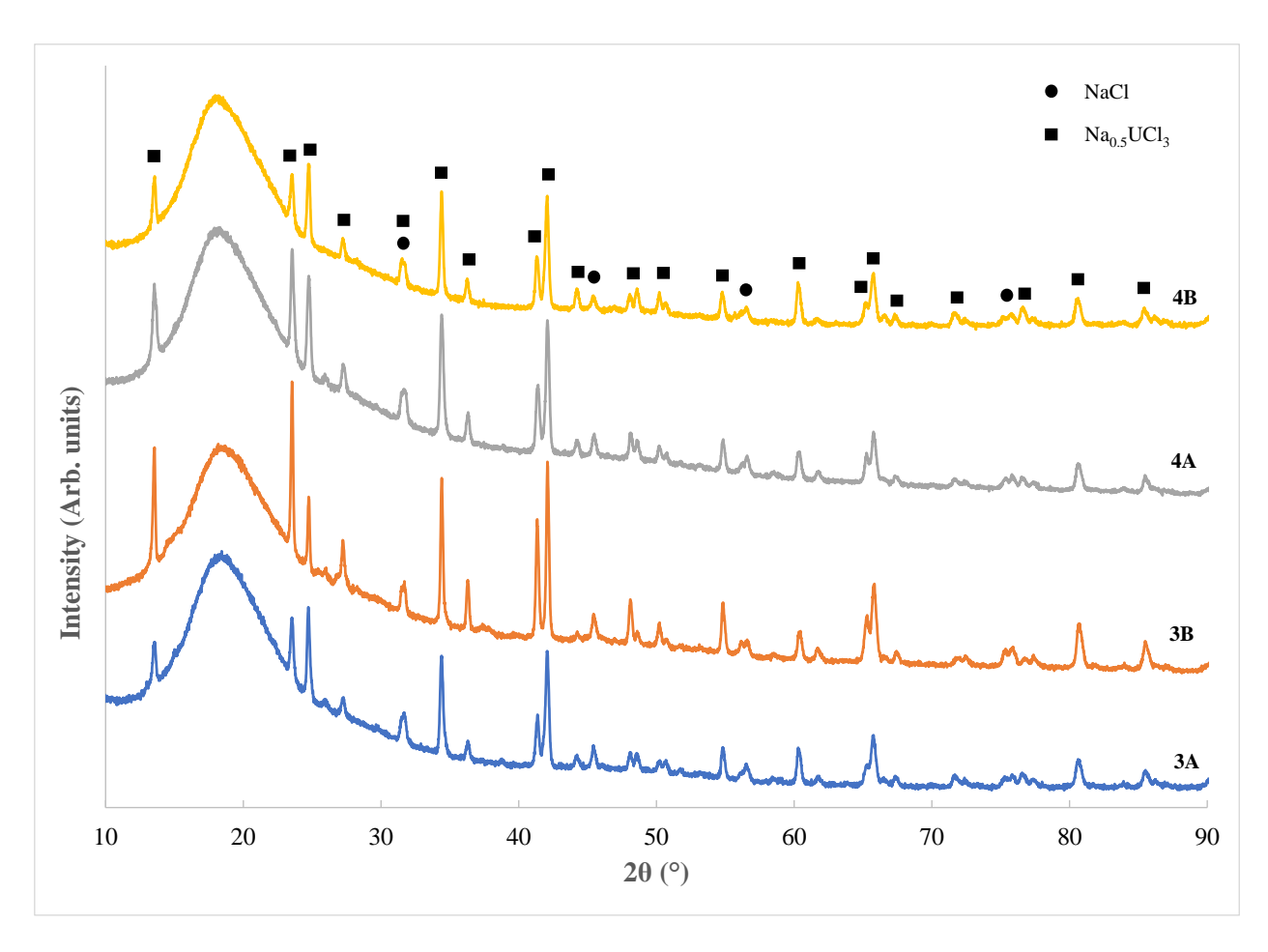


Figure 8. XRD patterns of sample material from runs 3 and 4.

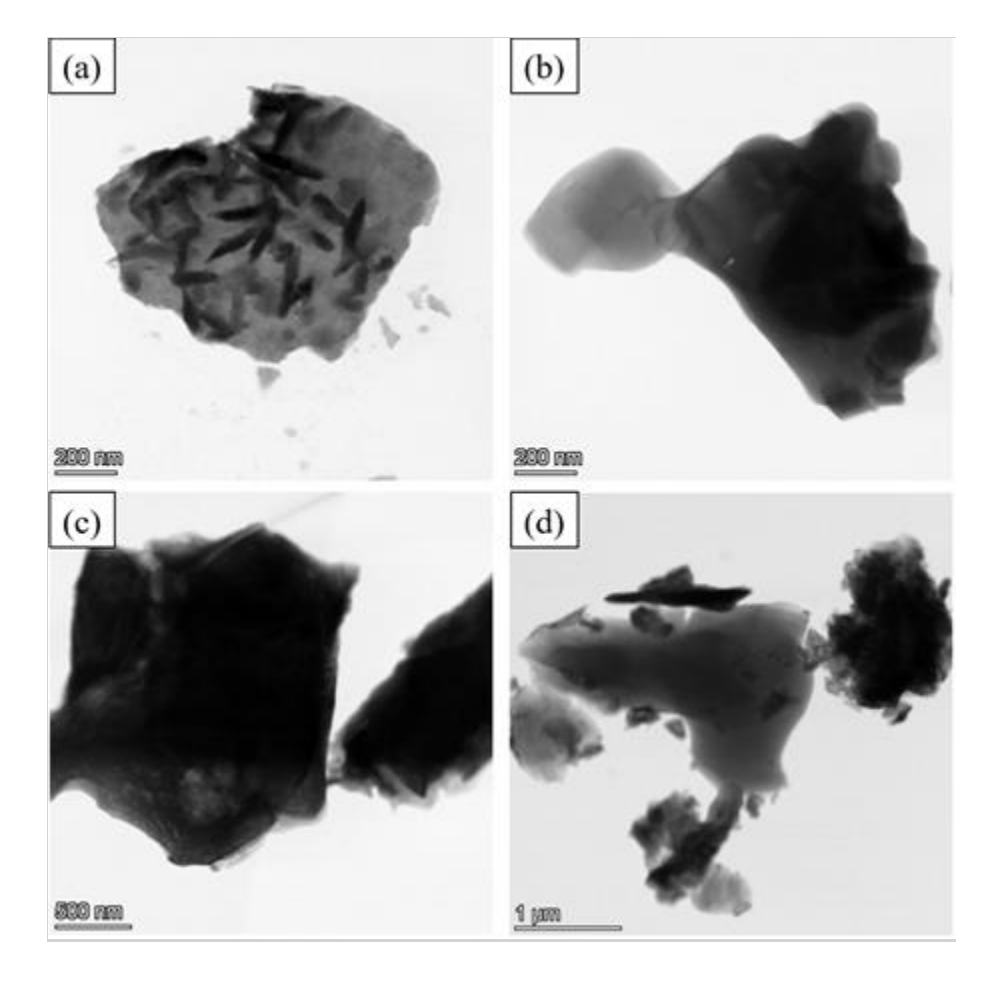


Figure 9. STEM images of samples (a) 1A, (b) 2A, (c) 3A, and (d) 4A.

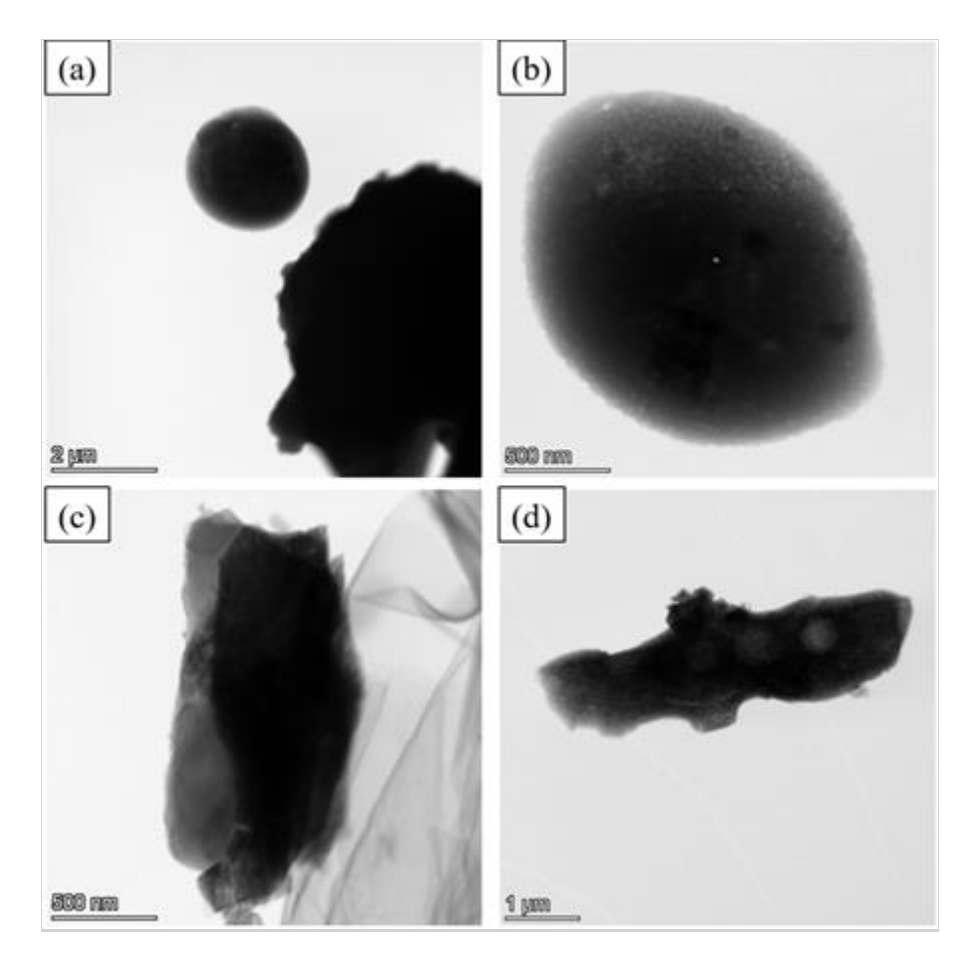


Figure 10. STEM images of samples (a) 1B, (b) 2B, (c) 3B, and (d) 4B.

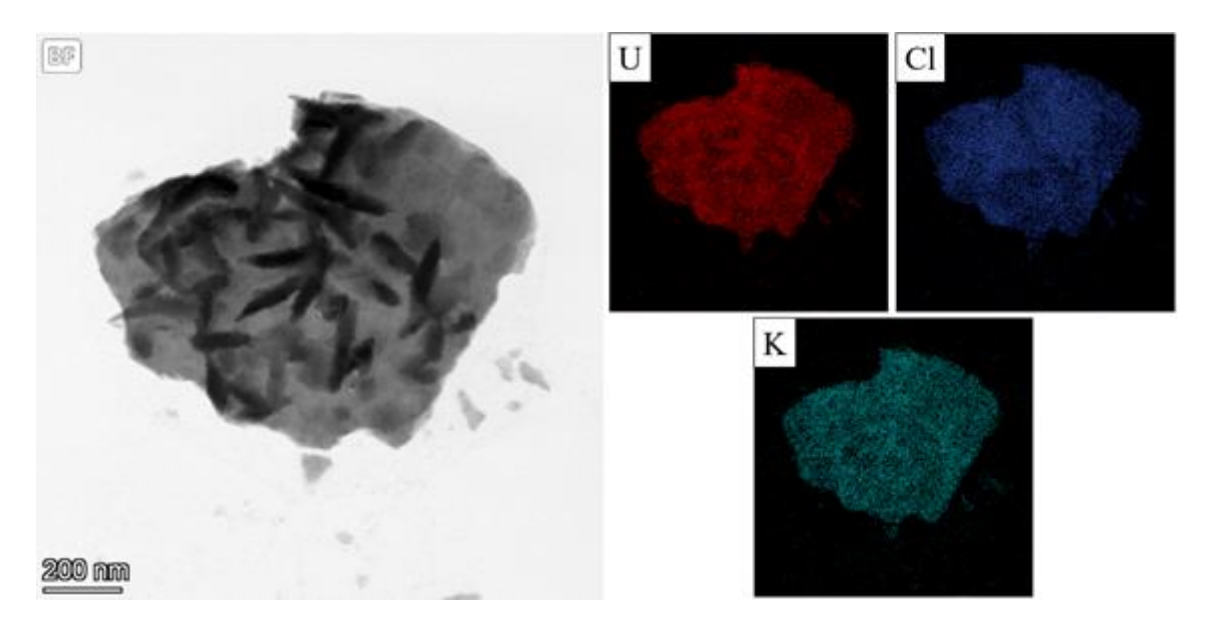


Figure 11. STEM-EDS map of sample 1A.